

Sonic Boom Alleviation Using Keel Configurations

Frank Marconi*

Allied Aerospace Industries, Ronkonkoma, New York 11779

Rodney D. W. Bowersox†

Texas A&M University, College Station, Texas 77843

and

Joseph A. Schetz‡

Virginia Polytechnic Institute and State University, Blacksburg, Virginia 24061

A detailed numerical investigation of the application of off-axis volume control for sonic boom mitigation is summarized. An 85-ft (25.9-m) aircraft flying at a Mach of 2.4 at an altitude of 57,000 ft (17.4 km) in a real atmosphere was studied. The off-axis volume was supplied by a keel system below the forward portion of the supersonic vehicle. The off-axis volume increased the fineness ratio of the vehicle by adding volume under the vehicle, thereby increasing its apparent length. A fully three-dimensional nonlinear Euler model was employed. The results presented proved that off-axis volume addition is effective and efficient for increasing the apparent length of the vehicle, thereby greatly alleviating sonic boom both on and off the flight-path axis. It was also shown that a keel swept forward normal to the Mach plane has a length efficiency factor equal to the freestream Mach number. It was further demonstrated that heat addition could be substituted for off-axis volume. Finally, nonlinear effects serve to minimize the keel size.

Nomenclature

A	=	airplane area distribution, $Kx^{5/2}$
K	=	5/2-area distribution strength
L	=	length
M	=	Mach number
p	=	pressure
R_b	=	body radius
r	=	radial coordinate
U	=	axial velocity
u	=	axial velocity perturbation
v	=	radial velocity perturbation
x	=	axial coordinate
y	=	curved characteristic line
β	=	$\sqrt{(M^2 - 1)}$
γ	=	ratio of specific heats
μ	=	Mach wave angle
ρ	=	density
ϕ	=	angle about the x axis, relative to the $-r$ axis

Subscripts

∞ = flight condition at altitude

Introduction

THE minimum achievable sonic boom from an aircraft is proportional to its weight divided by the 3/2 power of its length.^{1,2} This conclusion of the classical theory is the subject of little debate. The overpressure due to the lift needed to overcome the aircraft weight can not be avoided and is transmitted to the ground. In the case of

subsonic flight, this ground overpressure is spread over a long distance before and after the passing aircraft. In the case of supersonic flight, the overpressure can accumulate into two sudden jumps, that is, a sonic boom N wave. One approach to reduce the sonic boom is to increase the aircraft length to provide a larger distance over which the overpressures due to both lift and volume are spread. At a fixed lift and payload, that is, volume, as a supersonic vehicle's length is increased, so too is its fineness (diameter-to-length) ratio, which results in a decrease in wave drag. A decrease in wave drag is conceptually consistent with a decrease in sonic boom.

The possibility of eliminating shocks in the ground signature of a supersonic aircraft was first considered in detail by McLean,³ whose motivation was to achieve acceptable supersonic overflights. The acceptability of sonic booms with finite rise-time overpressures has been demonstrated in recent human subject tests.^{4,5} Sonic booms with rise times of about 10 ms and a realistic, 0.6-psf, overpressure were deemed acceptable by all of the subjects tested. Increasing the rise time reduces the acoustic power in the frequency range to which the ear is most sensitive. Linear theory indicates that the optimum shape for a finite rise time is a 5/2-power area distribution (that is, an isentropic spike), and the aircraft length required to achieve a 10-ms rise time has been proven to be impractical. McLean³ considered a supersonic transport (SST) class vehicle (600,000 lb, flying at 60,000 ft and Mach 2.7) and concluded that a length of 1000 ft was required. This was reduced substantially (to 570 ft) once atmospheric effects resulting in midfield signature freezing were included, but it is still considered impractical. Even the small (100,000-lb) vehicle considered in the present work requires about a 75% increase in length to achieve a 10-ms rise time (flying at a 57,000-ft altitude and Mach 2.4). Major structural dynamics problems are associated with such a long, slender vehicle.

The problems associated with building very long, slender, low-boom vehicles led researchers in the early 1970s (SST time frame) to consider exotic schemes for projecting the influence of a supersonic vehicle upstream. Miller and Carlson^{6,7} considered the projection of both a heat and a force field upstream of an SST class vehicle. Their work focused on projecting a "phantom body" in front of the SST, with the goal of a finite (10-ms) ground rise time. Using the one-dimensional equivalence between area and heat, they estimated that producing an equivalent (finite rise-time) length by such means would require nearly the same power as that needed to propel the vehicle.

Received 4 June 2002; revision received 11 November 2002; accepted for publication 12 November 2002. Copyright © 2003 by the American Institute of Aeronautics and Astronautics, Inc. All rights reserved. Copies of this paper may be made for personal or internal use, on condition that the copier pay the \$10.00 per-copy fee to the Copyright Clearance Center, Inc., 222 Rosewood Drive, Danvers, MA 01923; include the code 0021-8698/03 \$10.00 in correspondence with the CCC.

*Research Scientist, 77 Raynor Avenue. Associate Fellow AIAA.

†Associate Professor, Aerospace Engineering. Associate Fellow AIAA.

‡Professor and holder of the Fred D. Durham Endowed Chair, Aerospace and Ocean Engineering. Fellow AIAA.

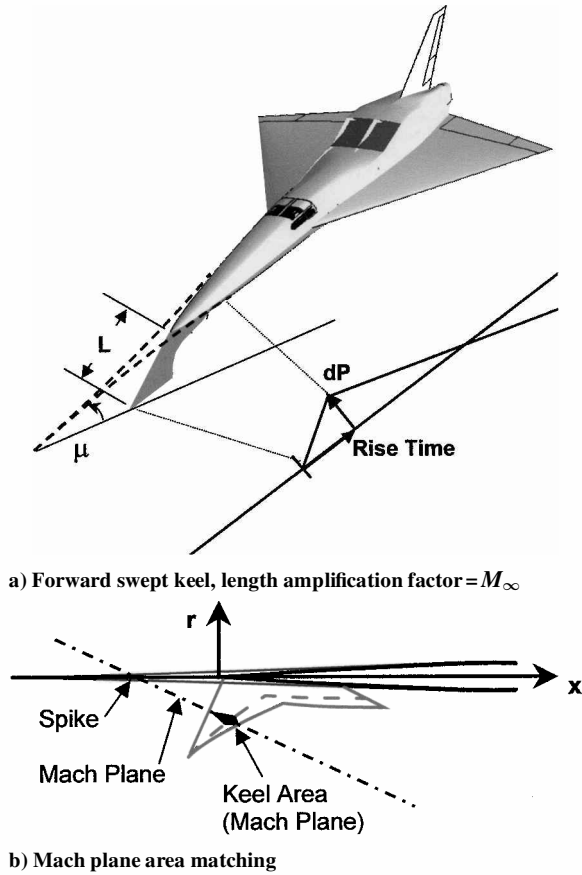


Fig. 1 Sonic boom mitigation concept.

The concept of an isentropic spike projected by energy addition was reconsidered by Marconi,⁸ where two-dimensional computational fluid dynamics (CFD) was used to evaluate the energy required. This study found the power requirements to be consistent with that of previous studies.^{6,7} A significant wave drag reduction was also found when the vehicle nose shock was replaced with an isentropic pressure rise.

There are a number of challenging problems associated with projecting energy upstream of a supersonic vehicle. Projection problems are avoided with the use of off-axis volume control as introduced by Batdorf.⁹ Figure 1a depicts his concept as implemented here by a forward-swept keel. Linear theory predicts that the asymptotic far-field flow is independent of the details of the vehicle and is influenced only by the cross-sectional area (and equivalent area due to lift) distribution of the configuration. In particular, in a supersonic flow, the cross-sectional area distribution in planes inclined at the Mach angle (μ in Fig. 1) governs the far-field flow downstream of those Mach planes. The theory predicts that whether the volume being cut is centered along the axis of the vehicle, that is, a nose spike, or shifted off-axis, that is, the keel in Fig. 1, should not influence the resulting far-field flow.

The first and very significant benefit of off-axis volume addition is a length amplification effect. In the optimum case of a keel swept forward normal to the Mach plane, a keel of length L can be used to produce the same effect as a spike of length $M_\infty \cdot L$. This amplification effect is significant. A second advantage of off-axis volume control, which was proposed by Batdorf,⁹ is that additional heat can be substituted for solid volume, that is, a thermal keel. Hanging a keel and burning jet fuel in its wake could be an efficient means of implementation, or the exhaust of a linear ramjet could possibly be tailored and used to mitigate sonic boom.

Batdorf's concept was tested by Swigart¹⁰ at Mach 2 and shown to be feasible. Swigart tested an equivalent body of revolution representing a typical SST with an all-solid keel in addition to a keel with a portion of its volume replaced by a heated region. He also tested a lifting wing-body combination with an all-solid keel. The keels

(both solid and thermal) were designed to match the Mach plane area of a 5/2-power isentropic spike and achieved a nearly linear near-field pressure distribution as expected. The solid keel tested by Swigart was very large, extending the entire length of the configuration. Only the thermal keel that was tested seemed practical. Furthermore, preliminary calculations performed by us indicated that a linear ramjet incorporated into the keel could facilitate this concept and potentially mitigate the drag and produce thrust.

The principal objective of this study was to further advance the keel concepts of Batdorf⁹ and Swigart¹⁰ using high-fidelity computational methods. Two representative equivalent bodies, with fineness ratios of 17:1 and 10:1, were examined. All of the results presented here assume a freestream Mach number of 2.4. The analyses for sonic boom mitigation were performed using a fully three-dimensional, nonlinear Euler model, where the initial spike sizing (Fig. 1a) was accomplished using a modified version of classical Whitham theory.¹¹ The spike-to-keel matching process is shown in Fig. 1b. A simple biwedge cross section was located in each Mach plane (dot-dash line in Fig. 1b) on the keel. The dashed line in Fig. 1b represents the maximum thickness location, and the biwedge keel area is indicated. The spike-to-keel transformation was found to be sensitive to the keel wedge angle. That is, it was difficult, due to nonlinear effects, to reproduce the spike flow with large keel half-angles. On the other hand, very thin keels are unacceptable from a manufacturing point of view. A 5.0-deg half-angle wedge was considered a reasonable compromise, and that was used as the baseline. However, for comparative purposes, a larger 10-deg wedge was also examined. The near-field pressure signatures were extrapolated to the ground using the methods in Refs. 12 and 13. In the propagation computations, an 85-ft vehicle flying at 57,000 ft in a real atmosphere was assumed. The following specific goals were pursued. First, off-flight-path sonic boom mitigation was examined. Second, techniques were developed and used to design thermal keel heating distributions. Third, the use of alternate keel orientations, length, and shape, to minimize overall size or produce tailored ground signatures, was examined. Fourth, multiple keel flowfields, for overall keel size reduction and improved off-axis mitigation, were studied.

Results and Discussion

Quasi-Linear Analysis

Seebass² presents an algorithm for using linear theory to predict sonic boom ground signatures. In summary, the midfield pressure signature is computed from the aircraft equivalent body of revolution using the quasi-linear theory of Whitham¹¹ making a large $\beta r/y$ far-field approximation, that is, computation of the F function. The midfield signature is then propagated to the ground using acoustic theory. A modified version of this theory (described next) was used for initial sizing of the phantom isentropic spike (dashed-lined-body extending forward of the airplane nose in Fig. 1).

In the present work, the far-field approximations in the classical Whitham theory¹¹ were relaxed; this was facilitated by the use of modern computational resources. Specifically, the small-disturbance perturbation velocity field solution, with the Whitham¹¹ modifications, to the linear form of the velocity potential equation,

$$\phi_{rr} + \phi_r/r - \beta^2 \phi_{xx} = 0 \quad (1)$$

is given by

$$\begin{aligned} \frac{u}{U_\infty} &= - \int_0^y \frac{f'(\eta) d\eta}{\sqrt{(y-\eta)(y-\eta+2\beta r)}} \\ \frac{v}{U_\infty} &= \frac{1}{r} \int_0^y \frac{(y-\eta+\beta r)f'(\eta) d\eta}{\sqrt{(y-\eta)(y-\eta+2\beta r)}} \end{aligned} \quad (2)$$

In Eq. (2), $y(x, r) = \text{const}$ is the nonlinear characteristic curve along which $dx/dr = \cot(\mu + \theta) \approx \beta + (\gamma + 1)M^4 u/2\beta - M^2(v + \beta u) + o(u^2 + v^2)$ (Ref. 11). Neglecting the second-order terms, substituting for the velocity components [Eq. (2)], and integrating $dx \approx [\beta + (\gamma + 1)M^4 u/2\beta - M^2(v + \beta u)]dr$ from the body

surface results in

$$x - \beta r =$$

$$\left\{ \begin{aligned} & -\frac{(\gamma+1)M_\infty^4}{2\beta^2} \int_0^y \frac{\sqrt{(y-\eta)+2\beta r} - \sqrt{y-\eta+2\beta R_B}}{\sqrt{y-\eta}} f'(\eta) d\eta \\ & -M_\infty^2 \left\{ \int_0^y \log \left[\frac{\sqrt{(y-\eta)+2\beta r} - \sqrt{y-\eta}}{\sqrt{(y-\eta)+2\beta r} + \sqrt{y-\eta}} \right] f'(\eta) d\eta \right. \\ & \left. - \int_0^y \log \left[\frac{\sqrt{(y-\eta)+2\beta R_B} - \sqrt{y-\eta}}{\sqrt{(y-\eta)+2\beta R_B} + \sqrt{y-\eta}} \right] f'(\eta) d\eta \right\} + y \end{aligned} \right. \quad (3)$$

Here $y(x, r)$ is the value of $x - \beta r$ where the characteristic meets the body surface; $f(x)$ represents the source distribution, and, when the tangency boundary condition is applied, $f(x) = A'(x)/2\pi$. Consistent with the small disturbance theory, the pressure field was computed from the linearized form of the compressible Bernoulli's equation ($p + \rho U^2 = \text{const}$)

$$(p - p_\infty)/p_\infty = -\gamma M_\infty^2 (u/U_\infty) \quad (4)$$

Using the preceding nonlinear characteristic theory improves the accuracy over traditional linear theory; however, multivalued solutions due to wave crossing (break points) are possible. Physically, the overlap regions correspond to coalescence of the Mach waves into a shock wave, followed by a discontinuous change in flow properties across the shock. Because near-field solutions ($r/L \sim 0.2$) were computed here, break points were rare, and, if they did occur, the spatial extent was very small. Hence, a simple shock-fitting algorithm similar to that of Whitham¹¹ was incorporated. The main simplification was that the shock was placed at the midpoint of the break region.

In summary, Eqs. (2–4), with 200 characteristics, were used to predict the velocity and pressure fields for a given airplane area distribution (with and without the phantom isentropic spikes), including the additional equivalent area due to lift. The integrals in Eq. (2) were evaluated using a fourth-order accurate numerical integration scheme; 5000 increments in η were used to ensure numerical convergence to within 0.1%. A computer program was written to perform this near-field analysis. The program was validated with the 5/2-power frontal spike experiment given by Swigart.¹⁰ A comparison of the present algorithm to the experimental data is shown in Fig. 2, and the agreement was considered satisfactory for the present sonic boom mitigation analysis.

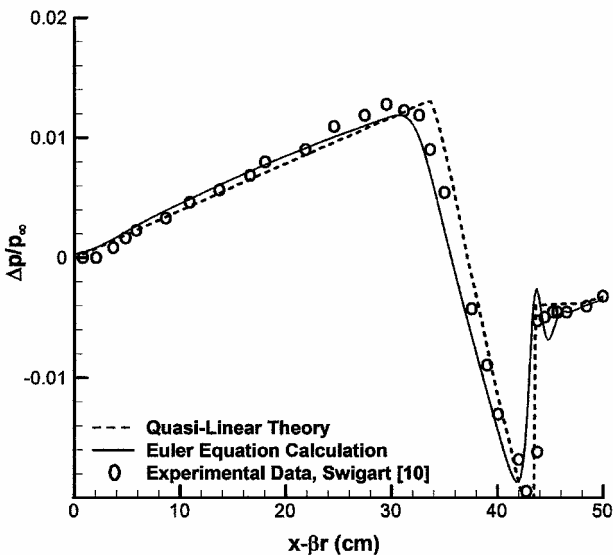


Fig. 2 Comparison of quasi-linear theory and Euler equation CFD with the frontal spike ($r = 50.8$ cm) data of Swigart.¹⁰

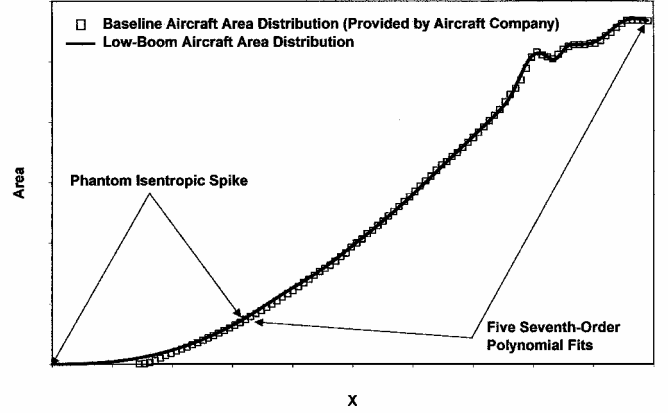


Fig. 3 Equivalent Mach plane area distribution with phantom isentropic spike and seventh-order polynomial splines (scales intentionally left blank).

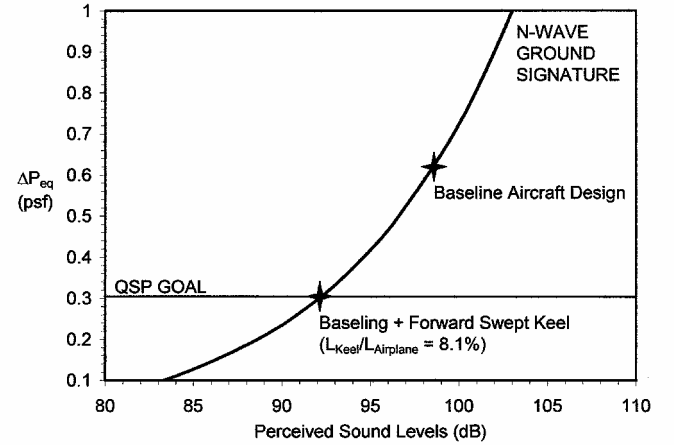


Fig. 4 Quasi-linear keel design to reduce the ground overpressure from the baseline aircraft to the quiet supersonic planform design goal of 0.3 psf.

The near-field solutions were extrapolated to the ground using the NASA Ames Research Center sonic boom FORTRAN routines in NFOO. In particular, the ANET¹² subroutine, which extrapolates the signal through the nonuniform atmosphere, was incorporated into the Whitham theory¹¹ program. A reflection factor of 1.9 was used, and wind effects were neglected. In addition, the perceived ground pressure levels were estimated with the PLdB¹³ subroutine also present in NFOO.

Phantom isentropic spikes (effectively extending the nose of the airplane in Figs. 1 and 2) were designed to lower the initial shock pressure rise to the design goal of 0.3 psf. The length and strength K of the 5/2-spike ($A = Kx^{5/2}$) were the design parameters. The spike was blended to the body, and the body geometry was fit with five, seventh-order polynomial curves. The coefficients were selected to ensure that the body fit was continuous through the third derivative. Figure 3 shows an example aircraft area distribution (including the equivalent area due to lift) with the isentropic (forward) spike and the body fits. This parameterization proved sufficient for all configurations tested. Because the 5/2-spike removes the discontinuous shock wave altogether, the perceived sound level (PLdB)⁴ was used to convert the linear ground signature waveform sound level into an equivalent shock wave signature, where the perceived sound levels were matched. Figure 4 shows an example result, where a spike was sized to reduce the initial shock pressure rise of just over 0.6 psf for the baseline aircraft down to 0.3 psf (the design goal). The length of the correspondingly swept forward keel would be 8.1% of the baseline aircraft length.

Nonlinear Analysis

The nonlinear design Euler procedure was initiated with a given spike (length and area distribution). In most cases, this was supplied

by the linear sizing scheme discussed in the preceding paragraphs. If the design goal was a linear profile with a finite ground rise time, then the 5/2-power area distribution was used, otherwise, a simple conical spike was used. The spike matched the baseline body and slope at a location depending on the baseline body and the spike. Sometimes, higher derivatives were matched. Given a chosen phantom spike, an all-solid keel was designed simply by matching the Mach plane area distribution of the spike.⁹ For the thermal keel, an aft portion of the area of the all-solid keel was replaced by heat addition. The first iteration for the heating distribution and accompanying area reduction was arrived at with the one-dimensional analysis discussed in Ref. 10. This heating distribution did not yield the desired pressure distribution, as predicted by the present three-dimensional nonlinear calculations, and so a series of design iterations using the three-dimensional CFD were performed.

The near-field ($r/L \sim 2.0$) pressure signatures were computed using the CFD code VULCAN¹⁴ run in an Euler space-marching mode. The heat was modeled using a source term in the energy equation. Grid convergence studies indicated that approximately 3 million grid points were required to capture all of the details of the flow accurately. This was considered to be a large number of points to resolve such a simple geometry, that is, a body of revolution with a keel; however, this grid was required to resolve the shock propagation far from the body. Furthermore, the grid lines were aligned almost parallel to the shock, and they were clustered in the neighborhood of the shock. The present Euler solution methodology was validated with the experimental data of Swigart¹⁰; a comparison is shown in Fig. 2. The NFBOOM code, with the parameters as listed earlier, was used to propagate the near-field pressures to the ground.

Solid and Thermal Keels

Given in Fig. 5 is the near-field pressure distribution one body length below a 17:1 fineness ratio body of revolution. The pressure ($p - p_\infty$)/ p_∞ is plotted vs an axial distance shifted to the origin of the disturbance, that is, the Mach line from the spike nose or keel tip, $x_0 = r / \tan(\mu) = \beta r$. The baseline body was fit with a 5/2-spike, and the baseline body-5/2-spike combination was simulated with the Euler solver to produce the target signature for the keel design. The pressure signature for the baseline body alone was also generated, and the trace is included in Fig. 5 for comparison purposes. With the target signature and phantom spike, a keel design process was performed. The pressure signature for the “converged” keel, with the aft portion replaced by heat (termed thermal keel), is also shown in Fig. 5. The heating distribution was controlled at four points in the base of the keel. The four numbered arrows in Fig. 5 represent the locations of heat control points; these, along with the final total temperature distribution, are shown relative to the keel in Fig. 6. The iteration was ad hoc, so that the target pressure distribution is arrived at only approximately. The iteration procedure took advantage of the

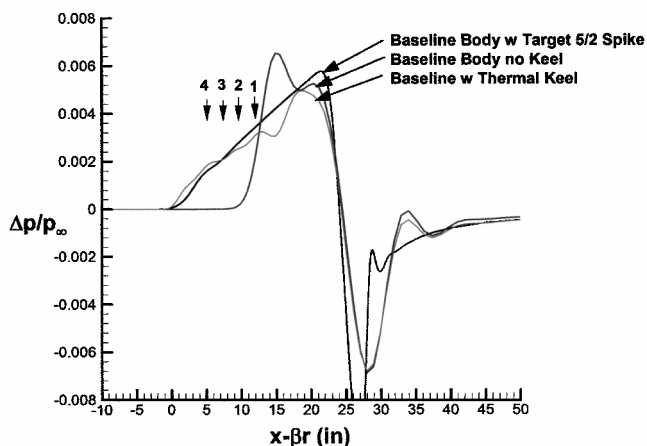


Fig. 5 Near-field pressure signatures one body length under the body for the 17:1 fineness ratio body (1–4 indicate the locations of the heat control points for the thermal keel).

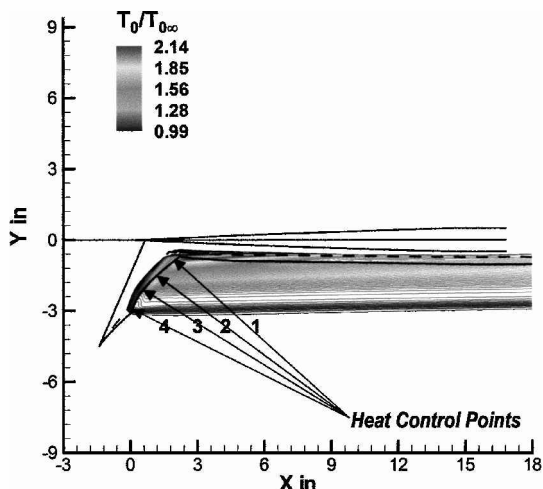


Fig. 6 Total temperature field, thermal keel on 17:1 baseline body and heating control point locations.

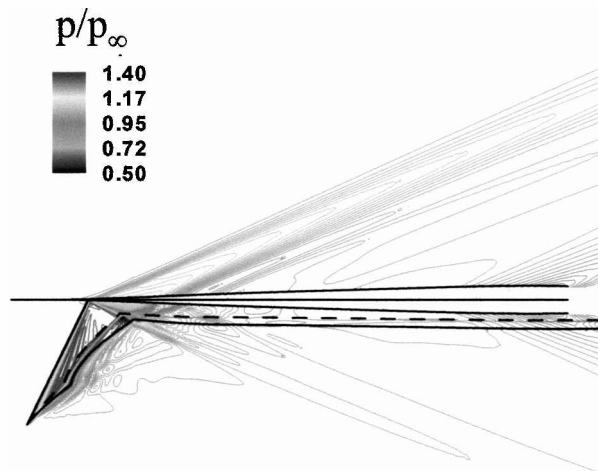


Fig. 7 Isobars in symmetry (flight-path) plane, 17:1 body with thermal keel.

supersonic nature of the flow by marching up the keel from control point number 4 to 1. The influence of each control point moves down along the slope of the local characteristics, so that once the pressure at point 4 (Fig. 5) converges to the target, the iteration is moved to point 3, keeping the heat at point 4 fixed. As indicated, the keel signature was in reasonable agreement with the target signature.

Given in Fig. 7 are the isobars in the symmetry (flight-path) plane; note the absence of a down-running shock. Shown in Fig. 8 is the corresponding pressure map in a transverse, vertical plane approximately one-half of a body length from the baseline body nose. The hole cut in the bottom of the shock by the keel is clear. The ground pressure signatures for the baseline body, the baseline body with the phantom spike, and the thermal keel under the flight path and 40 deg off of the flight path are presented in Fig. 9. The finite rise time (40 ms) of the spike is closely reproduced by the keel. Off of the flight path, two small shocks appear in the signature. Note that 40 deg off of the flight path is the worst location in this flowfield. Above 40-deg, natural boom mitigation dominates. In summary, all of the modified signatures shown in Fig. 9 are much more acceptable than that of the baseline body. An important conclusion from these results is that this single keel produced significant three-dimensional mitigation over the complete ground signature.

Forward Sweep

Sweeping the keel forward such that the leading edge of the keel is perpendicular to the freestream Mach line produces the minimum

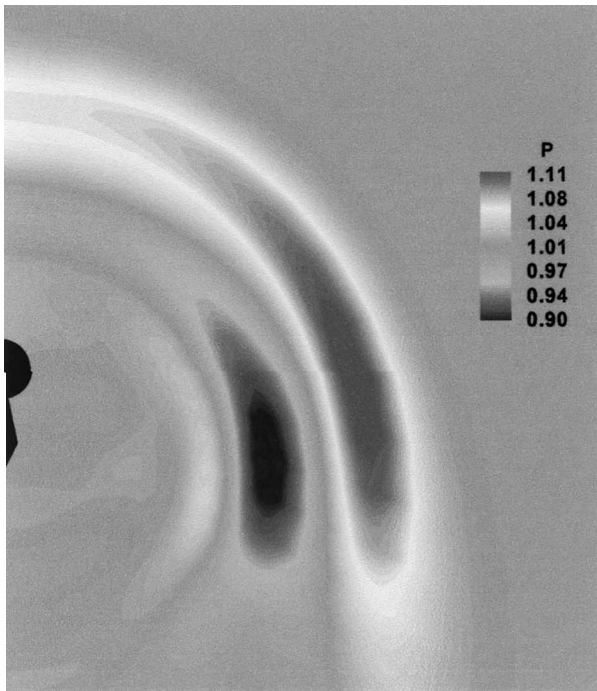


Fig. 8 Pressure map in plane at one-half body length, 17:1 body with thermal keel.

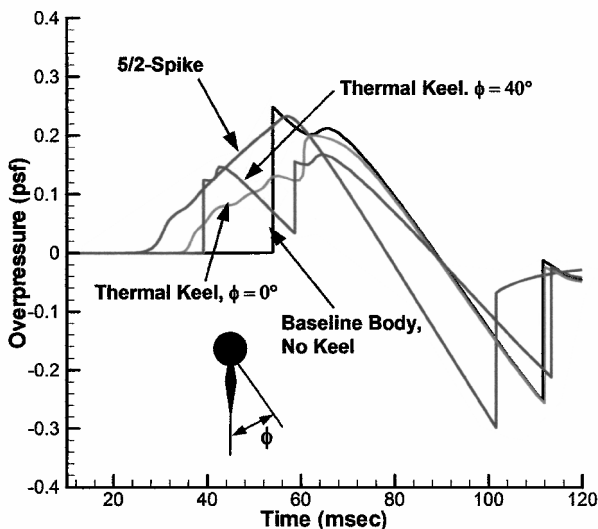


Fig. 9 Ground signature comparisons: 17:1 body, 5/2 spike, and thermal keel over and off of flight path.

length (vertically below the aircraft) device. The impact of sweeping the keel forward was investigated on a more realistic (in terms of baseline ground signature overpressure) 10:1 fineness ratio body. The results from this analysis are shown in Fig. 10. Specifically, the near-field pressure signatures (directly below the aircraft) for the baseline body, the baseline body with a 5/2 spike (target), a rear-swept (RS) keel based on the 5/2 area, and an equivalent forward-swept (FS) keel are compared. Note that the FS keel pressure seems to exhibit a small shock at about the location of the nose shock on the baseline body. This shock is typical and seems to originate at the corner (Fig. 11) of the FS keels. The corresponding ground signatures are shown in Fig. 12. The baseline body produced an initial shock rise of about 0.52 psf. The 5/2 spike replaced the shock with a linear pressure rise. The RS keel produced a signature that was roughly similar in shape to the 5/2 spike, albeit with some weak shocks (<0.1 psf). The FS keel replaced the single shock with two weaker shocks, each of which met the design goal of <0.3 psf.

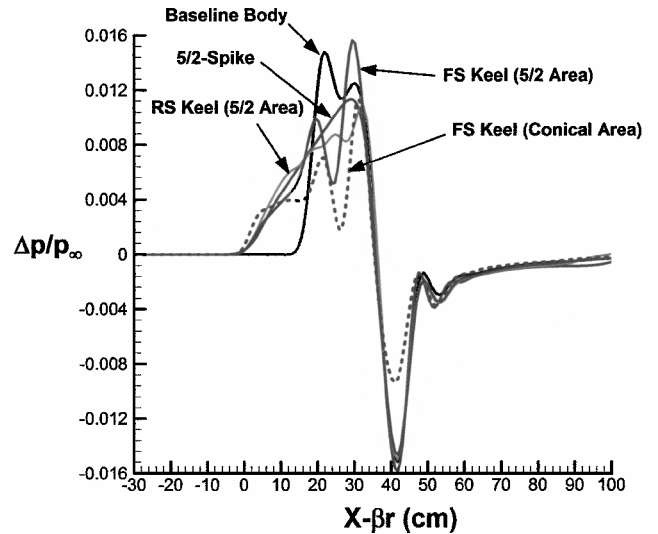


Fig. 10 Comparison of near-field pressures (one body length under equivalent body), 10:1 baseline body, RS and FS all-solid keels.

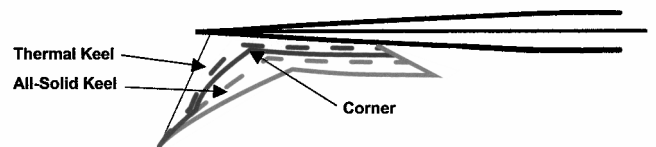


Fig. 11 Comparison between thermal keel and equivalent all-solid keel.

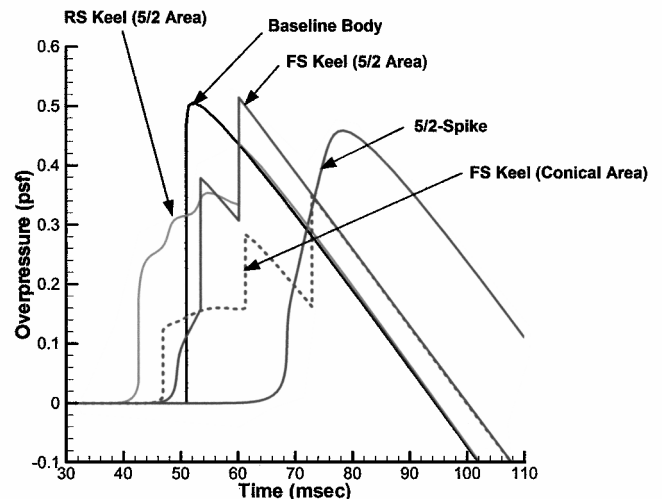


Fig. 12 Ground signature comparisons: 10:1 baseline body, RS and FS all-solid keels.

Conical Spike

The FS keel results shown in Figs. 10 and 12 provided the motivation for an alternate, easier to achieve, ground signature. Specifically, the linear finite rise-time ground signature of the 5/2 spike was abandoned and replaced with a series of weak shock waves. An FS keel designed to match the area of a simple conical spike was conceptualized and investigated. The near-field pressure signature for an FS keel with the area based on a simple conical spike is also plotted in Fig. 10. The corresponding ground signature is also shown in Fig. 12. The signature produced by the conical spike FS keel is very encouraging. The ground signatures produced by this keel at a number of stations to the side of the flight path are presented in Fig. 13, and, as indicated, all of the shocks in the ground signatures meet the design goal (0.3 psf).

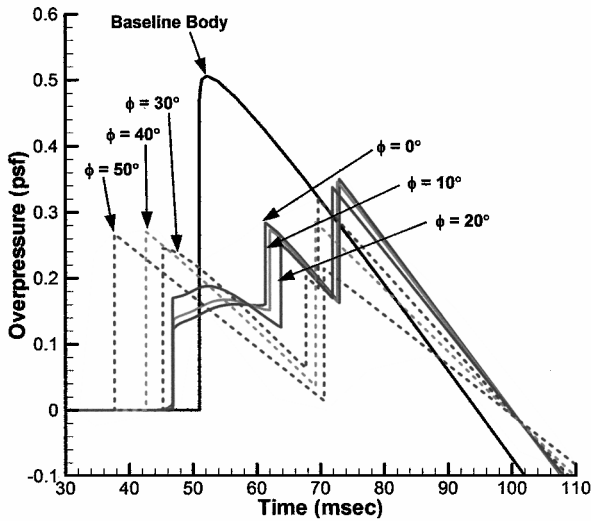


Fig. 13 Ground signatures off of flight path, 10:1 body FS all-solid keel to match a conical spike.

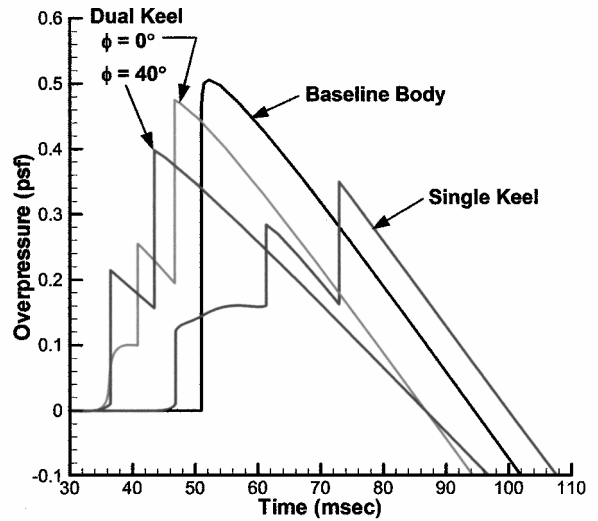


Fig. 15 Dual-keel (conical spike area divided by eight) and single-keel (full conical spike area) ground signatures.

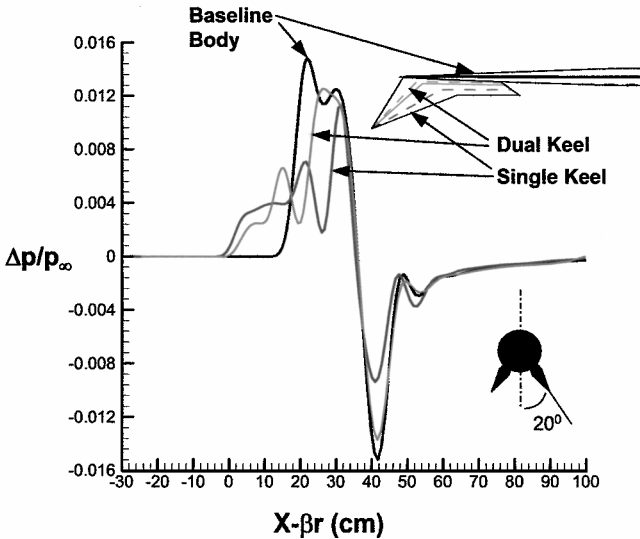


Fig. 14 Near-field pressure signatures and area distributions for the dual- and single-keel systems (10:1 baseline).

Dual Keels

In an attempt to improve the off-symmetry plane performance, a dual-keel system was devised. (See the insert in Fig. 14.) Here, the single symmetry plane keel is replaced by two keels 20 deg off of the symmetry plane. Linear theory would require that each of the two keels have exactly one-half of the sectional area of the phantom conical spike that they are replacing. It was found here that beneficial nonlinear interactions reduced the required area substantially. Presented in Fig. 14 are the near-field pressure produced by a two-keel system, where each had one-eighth of the area of a single, symmetry-plane keel. Although the pressure produced by the two keels does not match the single-keel pressure exactly, any addition to the two keel areas produced large increases in the pressure. Additional design iterations may result in a better near-field pressure. The corresponding ground signatures are plotted in Fig. 15, and, although the two-keel signatures (over the flight path and 40 deg off) exhibit stronger shocks than the single keel, the results were still within the 0.3-psf design goal. The insert in the upper-right corner of Fig. 14 compares the planforms of the single- and dual-keel configurations.

10-Degree Biwedge

To further reduce the planform area, the keel length was reduced by 25%, and the section half-angle was doubled to 10 deg. The results are shown in Figs. 16 and 17, where the insert in Fig. 16

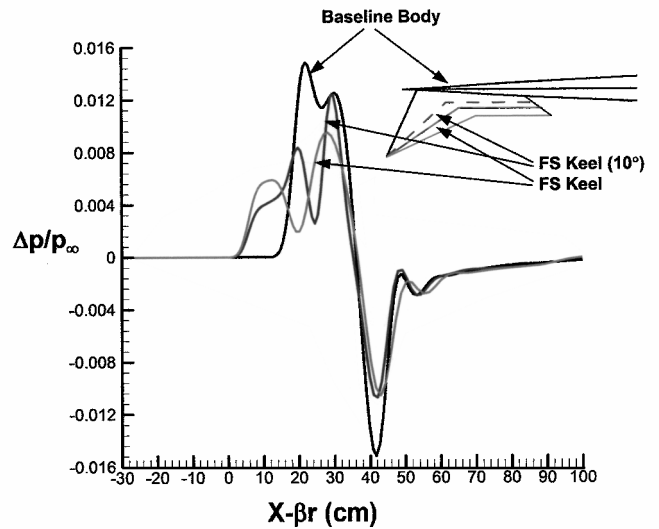


Fig. 16 Planform reduction resulting from increased section angle; short keel (75% conical area) on 10:1 baseline body.

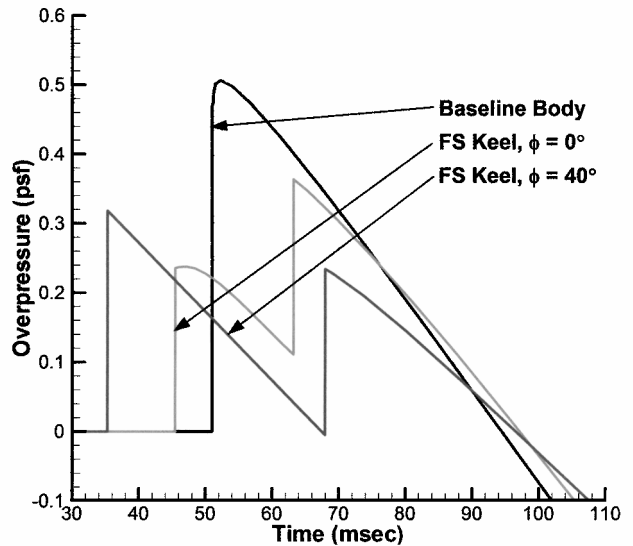


Fig. 17 Ground signatures for the 10-deg section keel.

shows the planform area reduction. The near-field pressure signatures in Fig. 16 show that the length over which the pressure rises was reduced proportionally to the keel length. Compare corresponding plots in Figs. 14 and 16. The impact on the ground signature is shown in Fig. 17. The three-shock signature in Fig. 13 or 15 was replaced by a two-shock signature due to coalescence. Each shock still meets the design goal of 0.3 psf. The shock off of the flight path was only slightly above the design limit.

Conclusions

A detailed numerical investigation of the use of off-axis volume control for sonic boom mitigation was performed. The concept studied here increased the apparent fineness ratio of a vehicle by adding volume under the vehicle, thereby increasing its apparent length. The off-axis volume was supplied by a keel system below the forward portion of the vehicle. As such, the off-axis volume was designed to match the Mach plane area of a slender nose spike. The analysis utilized fully three-dimensional, nonlinear, inviscid CFD and a modified near-field version of Whitham's¹¹ quasi-linear theory to analyze and better understand the mitigation phenomena. The results presented here prove that off-axis volume addition is effective and efficient in increasing the apparent length of a vehicle, thereby greatly alleviating sonic boom. The following specific conclusions were also drawn. First, the thin single keels produced significant three-dimensional mitigation over the entire ground signature. Second, heat addition, that is, the thermal keel, was shown to be effective in reducing the size of the all-solid keel. Third, sweeping the keels forward to minimize the vertical length below the aircraft was found to be viable. Fourth, it was demonstrated that the nonlinear effects associated with dual-keel configurations or thick section keels have the potential to reduce the keel size.

Acknowledgments

This work was sponsored under Agreement Number MDA972-01-005 by the Defense Advanced Research Projects Agency (DARPA). The DARPA Program Manager was Richard Wlezien.

The authors gratefully acknowledge this support. In addition, the authors acknowledge the support of Jeffrey White (NASA Langley Research Center) and Donald Durston (NASA Ames Research Center) in conjunction with the VULCAN and NFBOOM codes, respectively.

References

- ¹Seebass, R., and Argrow, B., "Sonic Boom Minimization Revisited," AIAA Paper 98-2956, June 1998.
- ²Seebass, R., "Sonic Boom Theory," *Journal of Aircraft*, Vol. 6, No. 3, 1969, pp. 177-184.
- ³McLean, E., "Configuration Design for Specific Pressure Signature Characteristics," NASA SP-180, May 1968, pp. 37-45.
- ⁴Leatherwood, J. D., and Sullivan, B. M., "Laboratory Study of Sonic Boom Shaping on Subjective Loudness and Acceptability," NASA TP-3269, Oct. 1992.
- ⁵McCurdy, D. A., "Subjective Response to Sonic Booms Having Different Shapes, Rise Times, and Duration," NASA TM 109090, March 1994.
- ⁶Miller, D. S., and Carlson, H. W., "A Study of the Application of Heat or Force Field to the Sonic-Boom-Minimization Problem," NASA TND-5582, Dec. 1969.
- ⁷Miller, D. S., and Carlson, H. W., "On the Application of Heat or Force Field to the Sonic-Boom-Minimization Problem," AIAA Paper 70-903, July 1970.
- ⁸Marconi, F., "An Investigation of Tailored Upstream Heating for Sonic Boom and Drag Reduction," AIAA Paper 98-0333, Jan. 1998.
- ⁹Batdorf, S. B., "On Alleviation of the Sonic Boom by Thermal Means," AIAA Paper 70-1323, Oct. 1970.
- ¹⁰Swigart, R. J., "Verification of the Heat-Field Concept for Sonic-Boom Alleviation," *Journal of Aircraft*, Vol. 12, No. 2, 1975, pp. 66-71.
- ¹¹Whitham, G., "The Flow Pattern of a Supersonic Projectile," *Communications on Pure and Applied Mathematics*, Vol. 5, 1952, pp. 301-348.
- ¹²Thomas, C., "Extrapolation of Sonic Boom Pressure Signatures by the Waveform Parameter Method," NASA TN D-6832, June 1972.
- ¹³Shepard, K., and Sullivan, B., "A Loudness Calculation Procedure Applied to Shaped Sonic Booms," NASA TP 3134, Nov. 1991.
- ¹⁴White, J. A., and Morrison, J. A., "A Pseudo-Temporal Multi-Grid Relaxation Scheme for Solving the Parabolized Navier-Stokes Equations," AIAA Paper 99-3360, Jan. 1999.